ISSN 1007-9327 (print)
ISSN 2219-2840 (online)

World Journal of *Gastroenterology*

World J Gastroenterol 2019 April 28; 25(16): 1907-2018

Published by Baishideng Publishing Group Inc

World Journal of Gastroenterology

Contents

Weekly Volume 25 Number 16 April 28, 2019

CASE REPORT

ABOUT COVER

Editorial board member of *World Journal of Gastroenterology*, Gwang Ha Ha Kim, MD, PhD, Full Professor, Department of Internal Medicine, Pusan National University School of Medicine, Busan 49241, South Korea

AIMS AND SCOPE

World Journal of Gastroenterology (*World J Gastroenterol*, *WJG*, print ISSN 1007-9327, online ISSN 2219-2840, DOI: 10.3748) is a peer-reviewed open access journal. The *WJG* Editorial Board consists of 642 experts in gastroenterology and hepatology from 59 countries.

The primary task of *WJG* is to rapidly publish high-quality original articles, reviews, and commentaries in the fields of gastroenterology, hepatology, gastrointestinal endoscopy, gastrointestinal surgery, hepatobiliary surgery, gastrointestinal oncology, gastrointestinal radiation oncology, *etc*. The *WJG* is dedicated to become an influential and prestigious journal in gastroenterology and hepatology, to promote the development of above disciplines, and to improve the diagnostic and therapeutic skill and expertise of clinicians.

INDEXING/ABSTRACTING

The *WJG* is now indexed in Current Contents®/Clinical Medicine, Science Citation Index Expanded (also known as SciSearch®), Journal Citation Reports®, Index Medicus, MEDLINE, PubMed, PubMed Central, Scopus and Directory of Open Access Journals. The 2018 edition of Journal Citation Report® cites the 2017 impact factor for *WJG* as 3.300 (5-year impact factor: 3.387), ranking *WJG* as 35th among 80 journals in gastroenterology and hepatology (quartile in category Q2).

RESPONSIBLE EDITORS FOR THIS ISSUE

Responsible Electronic Editor: *Han Song* **Proofing Editorial Office Director:** *Ze-Mao Gong*

NAME OF JOURNAL
World Journal of Gastroenterology

ISSN
ISSN 1007-9327 (print) ISSN 2219-2840 (online)

LAUNCH DATE
October 1, 1995

FREQUENCY
Weekly

EDITORS-IN-CHIEF
Subrata Ghosh, Andrzej S Tarnawski

EDITORIAL BOARD MEMBERS
http://www.wjgnet.com/1007-9327/editorialboard.htm

EDITORIAL OFFICE
Ze-Mao Gong, Director

PUBLICATION DATE
April 28, 2019

INSTRUCTIONS TO AUTHORS
https://www.wjgnet.com/bpg/gerinfo/204

GUIDELINES FOR ETHICS DOCUMENTS
https://www.wjgnet.com/bpg/GerInfo/287

GUIDELINES FOR NON-NATIVE SPEAKERS OF ENGLISH
https://www.wjgnet.com/bpg/gerinfo/240

PUBLICATION MISCONDUCT
https://www.wjgnet.com/bpg/gerinfo/208

ARTICLE PROCESSING CHARGE
https://www.wjgnet.com/bpg/gerinfo/242

STEPS FOR SUBMITTING MANUSCRIPTS
https://www.wjgnet.com/bpg/GerInfo/239

ONLINE SUBMISSION
https://www.f6publishing.com

World Journal of Gastroenterology

Submit a Manuscript: https://www.f6publishing.com

World J Gastroenterol 2019 April 28; 25(16): 1986-1996

DOI: 10.3748/wjg.v25.i16.1986

ISSN 1007-9327 (print) ISSN 2219-2840 (online)

ORIGINAL ARTICLE

Retrospective Study

Dual energy computed tomography for detection of metastatic lymph nodes in patients with hepatocellular carcinoma

Yu-Rong Zeng, Qi-Hua Yang, Qing-Yu Liu, Jun Min, Hai-Gang Li, Zhi-Feng Liu, Ji-Xin Li

ORCID number: Yu-Rong Zeng (0000000266977709); Qi-Hua Yang (0000-0003-1631-9940); Qing-Yu Liu (0000000171716346); Jun Min (0000-0001-6380-3351); Hai-Gang Li (0000-0002-6687-8874); Zhi-Feng Liu (0000-0002-1807-9576); Ji-Xin Li (0000-0002-8842-8647).

Author contributions: Zeng YR and Yang QH contributed equally to this work; Zeng YR, Yang QH, and Liu QY designed the research; Zeng YR, Yang QH, Min J, Li HG, and Liu ZF performed the research; Li JX contributed technical guidance and operation; Zeng YR, Yang QH, Min J, and Liu ZF analyzed the data; Zeng YR, Yang QH, and Liu QY wrote the paper.

Institutional review board statement: The study was reviewed and approved by the institutional review board of Sun Yat-sen Memorial Hospital.

Informed consent statement: Informed consent was waived by the ethics committee of Sun Yat-sen Memorial Hospital.

Conflict-of-interest statement: There is no conflict of interest associated with any of the senior author or other coauthors who contributed their efforts in this manuscript.

Yu-Rong Zeng, Qi-Hua Yang, Qing-Yu Liu, Ji-Xin Li, Department of Radiology, Sun Yat-sen Memorial Hospital, Sun Yat-sen University, Guangzhou 510120, Guangdong Province, China

Jun Min, Department of Hepatobiliary Surgery, Sun Yat-sen Memorial Hospital, Sun Yat-sen University, Guangzhou 510120, Guangdong Province, China

Hai-Gang Li, Department of Pathology, Sun Yat-sen Memorial Hospital, Sun Yat-sen University, Guangzhou 510120, Guangdong Province, China

Zhi-Feng Liu, Department of Radiology, Zengcheng District People's Hospital of Guangzhou, Guangzhou 511300, Guangdong Province, China

Corresponding author: Qing-Yu Liu, PhD, Attending Doctor, Professor, Department of Radiology, Sun Yat-sen Memorial Hospital, Sun Yat-sen University, 107 West Yanjiang Road, Guangzhou 510120, Guangdong Province, China. liuqy@mail.sysu.edu.cn
Telephone: +86-13694201711
Fax: +86-20-81332702

Abstract

BACKGROUND

Regional lymph node metastasis in patients with hepatocellular carcinoma (HCC) is not uncommon, and is often under- or misdiagnosed. Regional lymph node metastasis is associated with a negative prognosis in patients with HCC, and surgical resection of lymph node metastasis is considered feasible and efficacious in improving the survival and prognosis. It is critical to characterize lymph node preoperatively. There is currently no consensus regarding the optimal method for the assessment of regional lymph nodes in patients with HCC.

AIM

To evaluate the diagnostic value of single source dual energy computed tomography (CT) in regional lymph node assessment for HCC patients.

METHODS

Forty-three patients with pathologically confirmed HCC who underwent partial hepatectomy with lymphadenectomy were retrospectively enrolled. All patients underwent dual-energy CT preoperatively. Regional lymph nodes (n = 156) were divided into either a metastatic (group P, n = 52) or a non-metastasis group (group N, n = 104), and further, according to pathology, divided into an active hepatitis (group $P1$, n = 34; group $N1$, n = 73) and a non-active hepatitis group (group $P2$, n = 18; group $N2$, n = 31). The maximal short axis diameter (MSAD), iodine concentration (IC), normalized IC (NIC), and the slope of the spectral

Manuscript source: Unsolicited manuscript

Received: February 2, 2019
Peer-review started: February 6, 2019
First decision: March 5, 2019
Revised: March 14, 2019
Accepted: March 24, 2019
Article in press: March 24, 2019
Published online: April 28, 2019

P-Reviewer: Aghakhani A, Bramhall S, Köksal AS
S-Editor: Yan JP
L-Editor: Wang TQ
E-Editor: Song H

curve (λ_{HU}) of each group in the arterial phase (AP), portal phase (PP), and delayed phase (DP) were analyzed.

RESULTS

Analysis of the MSAD, IC, NIC, and λ_{HU} showed statistical differences between groups *P* and *N* ($P < 0.05$) during all three phases. To distinguish benign from metastatic lymph nodes, the diagnostic efficacy of IC, NIC, and λ_{HU} in the PP was the best among the three phases (AP, PP, and DP), with a sensitivity up to 81.9%, 83.9%, and 81.8%, and a specificity up to 82.4%, 84.1% and 84.1%, respectively. The diagnostic value of combined analyses of MSAD with IC, NIC, or λ_{HU} in the PP was superior to the dual energy CT parameters alone, with a sensitivity up to 84.5%, 86.9%, and 86.2%, and a specificity up to 83.0%, 93.6% and 89.8%, respectively. Between groups *P1* and *P2* and groups *N1* and *N2*, only IC, NIC, and λ_{HU} between groups *N1* and *N2* in the PP had a statistically significant difference ($P < 0.05$).

CONCLUSION

Dual-energy CT contributes beneficially to regional lymph node assessment in HCC patients. Combination of MSAD with IC, NIC, or λ_{HU} values in the PP is superior to using any single parameter alone. Active hepatitis does not deteriorate the capabilities for characterization of metastatic lymph nodes.

Key words: Computed tomography; Hepatocellular carcinoma; Lymph node; Metastasis; Hepatitis; Dual energy

Core tip: Dual-energy computed tomography (CT) contributes beneficially to regional lymph node assessment in hepatocellular carcinoma (HCC) patients, which can differentiate metastatic and non-metastatic lymph nodes for improving regional lymph node staging of HCC. Combination of maximal short axis diameter with dual-energy CT quantifiable parameters (iodine concentration, normalized iodine concentration, or the slope of the spectral curve) in the portal phase can be more advantageous in regional lymph node assessment. Active hepatitis does not deteriorate the detection and characterization of metastatic lymph nodes in HCC.

Citation: Zeng YR, Yang QH, Liu QY, Min J, Li HG, Liu ZF, Li JX. Dual energy computed tomography for detection of metastatic lymph nodes in patients with hepatocellular carcinoma. *World J Gastroenterol* 2019; 25(16): 1986-1996
URL: https://www.wjgnet.com/1007-9327/full/v25/i16/1986.htm
DOI: https://dx.doi.org/10.3748/wjg.v25.i16.1986

INTRODUCTION

Regional lymph node metastasis in patients with hepatocellular carcinoma (HCC) is not uncommon. Although it is found in only 8% of cases at the time of hepatectomy[1], in autopsies it has been reported to be as high as 26% to 37%[1], suggesting that lymph node metastases are often under- or misdiagnosed[2,3]. Regional lymph node metastasis is associated with a negative prognosis in patients with HCC[3,4], as the incidence of lymph node metastasis usually indicates an advanced tumor stage with infiltration of blood vessels[2]. Even with aggressive treatment such as radical resection, the reported median survival rate is much lower than that for patients without lymph node metastasis (28 mo *vs* 53 mo), and the tumor recurrence rate (a median follow-up of 43 mo) is significantly higher (82.05% *vs* 57.64%)[1-3,5]. Although effective treatment for metastatic lymph nodes of HCC has not yet been established[6], surgical resection of lymph node metastasis is considered feasible and efficacious in improving the survival and prognosis of patients with HCC[1,2,4,6].

There is currently no consensus regarding the optimal method for the assessment of regional lymph nodes in patients with HCC[7]. The diagnostic criteria of conventional computed tomography (CT) and magnetic resonance imaging (MRI) scans for differentiating malignant and benign lymph nodes were established according to size

(maximal short axis diameter ≥ 10 mm)[7,8]. However, it may be inaccurate in detecting metastatic lymph nodes in HCC, as over 80% of HCC patients in China have chronic hepatitis B virus (HBV) infection[9,10], and it is well documented that patients with chronic hepatitis or cirrhosis also have benign enlarged lymph nodes[10,11]. Diffusion-weighted MRI is sensitive in detecting metastatic lymph nodes, but it is easily affected by physical motion of the abdomen, and the accuracy will be lower (as low as 76%) when metastatic lymph nodes show necrosis[12]. ^{18}F-fluoro deoxyglucose-positron emission tomography/CT (^{18}F-FDG-PET/CT) is a non-invasive method for diagnosing lymph node metastasis, but it is expensive, low in spatial resolution[13,14], and can give false positive results[13,15,16]. Additionally, for lymph node metastases in HCC, the diagnostic value of a ^{18}F-FDG-PET/CT scan is lower than conventional imaging modalities[13]. Therefore, it is critical to explore better techniques for lymph node assessment in HCC patients.

Dual-energy CT can provide quantitative information with monochromatic spectral images, material decomposition images, spectrum curves, and effective atomic number images, based on the principle that different materials have their own characteristic X-ray absorption coefficient, combined with the technology of instantaneously switching 80/140 kVp (kilovolt peak) voltage[17]. The role of dual-energy CT in the evaluation of malignant lymph nodes in colorectal cancer, gynecological malignancies, hypopharyngeal cancer, and lung cancer has been reported[18-23]. However, there have been no dual-energy CT studies regarding lymph node assessment in HCC. The objective of this study was to evaluate the diagnostic value of dual-energy CT in preoperative lymph node assessment for HCC patients.

MATERIALS AND METHODS

Patients

This retrospective study was approved by the institutional review board of Sun Yat-sen Memorial Hospital. In this study, we conducted searches in a Picture Archiving and Communication System for patients suspected of having HCC and who underwent contrast-enhanced upper abdomen dual energy CT scans between July 2016 and November 2017. There were 153 patients identified with this search process, and among them 110 were excluded for the following reasons (Figure 1): Patients did not receive surgical treatment (n = 25), patients also had other malignant tumors (n = 3), patients underwent preoperative treatment of HCC (transarterial chemoembolization) (n = 11), pathology results confirmed a final diagnosis of non-HCC (n = 9), patients did not undergo lymphadenectomy or partial lymphadenectomy (n = 59), and patients did not have a CT re-examination within two weeks after surgery (n = 3). Ultimately, there were 43 patients (37 males and 6 females; median age of 51 years; 34 patients with HBV and 10 patients with liver cirrhosis; average size of resected tumor: 4.6 cm) enrolled in the study.

Dual-energy CT acquisition

CT scans were performed on a single source dual energy CT scanner (Discovery CT750 HD, GE Healthcare) with rapid KeV switching, including a pre-contrast CT plain scan and a post-contrast scan in the arterial phase (AP), portal phase (PP), and delayed phase (DP). The contrast enhanced scan began at 25 s (AP), 65 s (PP), and 180 s (DP) after the injection of Ioversol 320 (Optiray-Covidean) at a flow rate of 3 mL/s and an amount of 1.0 mL per kilogram of body weight. The scanning parameters were as follows: Tube current, 600 mA; tube voltage, 80/140 Kvp; tube rotation time, 0.8 s; pitch, 1.375:1; slice thickness, 1.25 mm; interval thickness, 1.25 mm. Further analysis of images was performed on a GE Advantage Workstation AW4.4 (GE Healthcare).

Image analysis

The image data of 43 patients with pathologically confirmed HCC were analyzed. Regional lymph nodes were measured independently by two radiologists with more than 10 years of experience. The radiologists were blinded to the pathological results (metastatic or non-metastatic) but were aware of the location of any removed lymph nodes. Lymph nodes with a short axis (≥ 4.0 mm), and which were confirmed in the resection range by comparing preoperative and postoperative CT images (performed within two weeks after operation), were all measured (Figure 2). A circle of region of interest (ROI) was manually drawn in the maximal axial section for lymph nodes, containing most of the lymph node volume as possible, and the average size of ROIs was larger than 12.0 mm^2. Measurements were repeated three times and the average values were recorded. The iodine (water)-based material decomposition images and monochromatic images (energy ranging from 40 to 140 keV with a 10 keV interval)

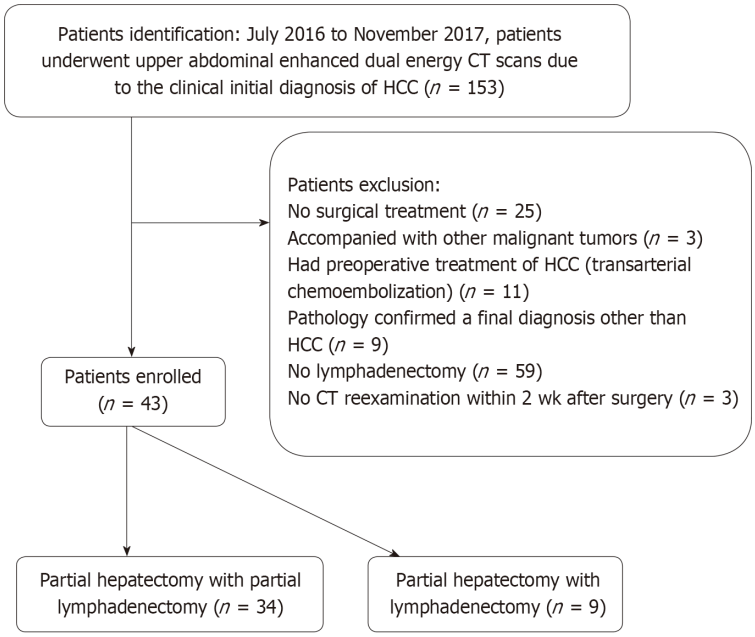

Figure 1 Patient identification and exclusion. HCC: Hepatocellular carcinoma; CT: Computed tomography.

were reconstructed and analyzed. The following parameters were all measured in the AP, PP, and DP: (1) Iodine concentrations (IC) (mg/mL), the average value of which was calculated on the iodine (water)-based material decomposition images; (2) normalized IC (NIC), which was a calculation of the IC of lymph nodes to the IC of the thoracic aorta on the same slice, namely NIC = IC/ICaorta; and (3) slope of the spectral curve (λ_{HU}), which was divided from the HU curve by the difference between the CT values at 40 keV and 80 keV (as the curve from 80 keV to 140 keV tends to be a horizontal line): $\lambda_{HU} = (HU_{40kev} - HU_{80Kev})/40$.

Pathology and clinical data analysis

The regional lymphadenectomy included the lymph nodes in the hepatic pedicle (including the cystic duct, peri-choledochal, hilar, periportal, and peri proper hepatic artery), retro-pancreatic space, common hepatic artery, and celiac trunk[2,5]. Partial lymphadenectomy restricted the extent of lymphadenectomy only to the suspected lymph nodes which were enlarged on CT images. Removed regional lymph nodes were categorized into groups according to the gastric cancer treatment guidelines of the Japanese Gastric Cancer Association[24] for pathological examination. The status of lymph nodes larger than 4.0 mm was reported pathologically. When the removed lymph nodes were pathologically confirmed to be metastatic, we included them in a metastatic group (group *P*), and when the removed lymph nodes were confirmed to be non-metastatic, they were classified into a non-metastatic group (group *N*).

Clinical data and laboratory results of biochemical blood examinations of all patients were collected. Active hepatitis was diagnosed according to the Chinese guidelines of prevention and treatment of viral hepatitis (2000)[25]. Patients who met one of the following conditions were considered to have active hepatitis: (1) Positive findings of epidemiological contact history, clinical presentation, and viral hepatitis pathogenic examination, with an elevated serum alanine aminotransferase (ALT) level; (2) patients with chronic hepatitis and who had symptoms of hepatitis again, with positive biochemical tests results (elevated serum ALT); or (3) a histopathological examination of the liver confirmed hepatitis. Patients who did not meet the above requirements were considered as having no active hepatitis.

Statistical analysis

Statistical analyses were performed with SPSS 17.0 (SPSS Inc.). Quantitative data are presented as median (P25, P75). Independent samples *t*-test was used for comparing normally distributed quantitative data in the two groups and a nonparametric test was applied when the data were not normally distributed or there was heterogeneity of variances. The diagnostic efficacies of the axial size, IC, NIC, and λ_{HU} for lymph nodes in the AP, PP, and DP were determined by the area under the curve (AUC) from the corresponding receiver operative characteristics (ROC) curves. A *P*-value ≤ 0.05 was considered statistically significant. Cut-off values, AUC, sensitivity, and

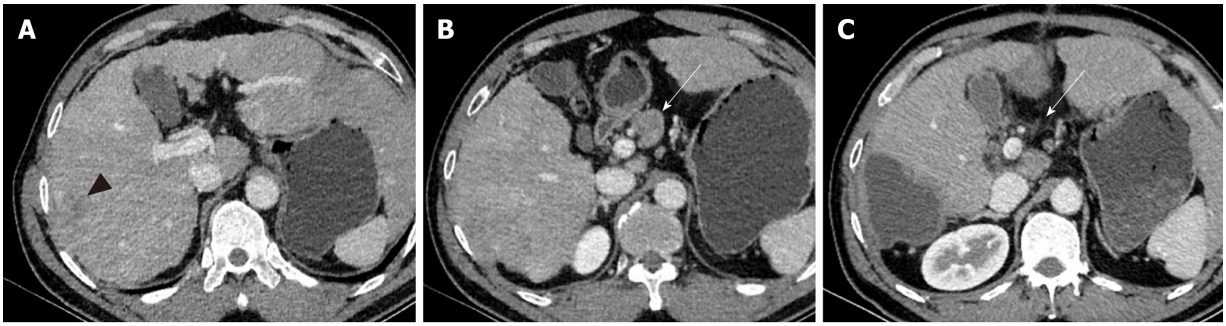

Figure 2 A 31-year-old male patient with hepatocellular carcinoma (black arrow head). A and B: Preoperative computed tomography (CT) scans in the portal phase; C: Postoperative CT scan in the portal phase. Preoperative and postoperative CT scans were compared to determine the location of the removed lymph node (white arrow). Pathology of this lymph node was benign. CT: Computed tomography.

specificity of DECT parameters (axial size, IC, NIC, and λ_{HU}) for metastatic *vs* non-metastatic lymph nodes in HCC were measured.

RESULTS

Lymph nodes

A total of 156 lymph nodes (104 non-metastatic and 52 metastatic) from 43 patients were finally included in this study. Among them, ten patients had a total of 52 lymph nodes which were pathologically proven to be metastatic and therefore divided into group *P*, while the other 33 patients with 104 total lymph nodes that were non-metastatic and thus divided into group *N*. According to the active hepatitis diagnosis standard described above, the lymph nodes in groups *P* and *N* were further divided into an active hepatitis group (group *P1*, $n = 34$; group *N1*, $n = 73$) and a non-active hepatitis group (group *P2*, $n = 18$; group *N2*, $n = 31$), respectively.

Maximal short axis diameter of lymph nodes

The mean maximal short axis diameter of group *P* (metastasis group) was significantly longer than that of group *N* (non-metastasis group) [1.25 (0.90, 1.80) *vs* 0.60 (0.50, 0.80), $P < 0.001$)] (Table 1). There was no significant difference between group *P1* (metastasis with active hepatitis) and group *P2* (metastasis with non-active hepatitis), or group *N1* (non-metastasis with active hepatitis) and group *N2* (non-metastasis with non-active hepatitis) (Table 2).

IC, NIC, and λ_{HU}

IC, NIC, and λ_{HU} values were significantly higher in group *P* than in group *N* in the AP, PP, and DP ($P < 0.05$) (Table 1), and they were also significantly higher in group *N1* than in group *N2* in the PP (Table 2). There were no significant differences in IC, NIC, or λ_{HU} values between groups *N1* and *N2* in the AP and DP, nor between groups *P1* and *P2* in the AP, PP, or DP (Table 2).

ROC analysis

The ROC curves of maximal short axis diameter, IC, NIC, and λ_{HU} in the AP, PP, and DP for diagnosing metastatic lymph nodes were drawn. The ROC curves of combination diagnoses using the four parameters (maximal short axis diameter, IC, NIC, and λ_{HU}) were also determined (Figure 3). The AUC, optimal cut-off value, sensitivity, and specificity of each single parameter and combined parameters for differentiating group *P* from group *N* are shown in Table 3. The optimal threshold of the maximal short axis diameter was 0.950 cm, with a sensitivity and specificity of 73.3% and 88.7%, respectively. The AUCs of IC, NIC, and λ_{HU} in the PP were the largest at an optimal threshold of 18.060 mg/mL, 0.272, and 1.098, respectively, with a sensitivity and specificity up to 81.9% and 82.4%, 83.9% and 84.1%, and 81.8% and 84.1%, respectively. The diagnostic efficacy of combination of the maximal short axis diameter with IC, NIC, or λ_{HU} in the PP (combined diagnosis in parallel) was superior to using a single parameter, with a sensitivity up to 84.5%, 86.9%, and 86.2%, and a specificity up to 83.0%, 93.6%, and 89.8%, respectively. The diagnostic efficacy of the maximal short axis diameter with NIC (PP) was the best (Figures 4 and 5).

Table 1 Quantitative parameters [median (P25, P75)] for metastatic *vs* non-metastatic lymph nodes in patients with hepatocellular carcinoma

Parameter		Metastatic (group *P*)	Non-metastatic (group *N*)	*P*-value
Maximal short axis diameter (cm)		1.25 (0.90, 1.80)	0.60 (0.50, 0.80)	< 0.001
IC (mg/mL)	AP	10.46 (9.41, 11.36)	8.64 (7.62, 9.82)	< 0.001
	PP	22.70 (19.08, 26.35)	13.26 (9.91, 16.26)	< 0.001
	DP	19.03 (16.18, 21.34)	14.09 (12.14, 15.71)	< 0.001
NIC	AP	0.12 (0.10, 0.13)	0.08 (0.06, 0.11)	< 0.001
	PP	0.54 (0.37, 0.82)	0.10 (0.07, 0.18)	< 0.001
	DP	0.57 (0.49, 0.77)	0.34 (0.23, 0.44)	< 0.001
λ_{HU}	AP	0.64 (0.57, 0.73)	0.49 (0.41, 0.58)	< 0.001
	PP	1.53 (1.26, 1.90)	0.87 (0.60, 0.94)	< 0.001
	DP	1.30 (1.15, 1.74)	0.85 (0.71, 1.40)	< 0.001

IC: Iodine concentration; NIC: Normalized iodine concentration; λ_{HU}: Slope of the spectral curve; AP: Arterial phase; PP: Portal phase; DP: Delayed phase.

DISCUSSION

In this study, we found that the parameters including maximal short axis diameter, IC, NIC, and λ_{HU} were significantly different between metastatic and non-metastatic lymph nodes in HCC patients. These parameters had favorable diagnostic value for identifying metastatic lymph nodes in the PP. The diagnostic efficacy was notably higher when using a combination of analysis of maximal short axis diameter with IC, NIC, or λ_{HU} values. The maximal short axis diameter of metastatic lymph nodes was longer than that of non-metastatic lymph nodes in the present study, with a diagnostic sensitivity of 73.3%, and a specificity of 88.7%. This finding is different from that of Grobmyer *et al*[7], who evaluated preoperative CT images of 236 lymph nodes in 100 patients with primary or secondary hepatic malignancies and found that the positive predictive value of diameter of lymph nodes was as low as 39%. Thus, the diagnostic efficacy of short axis diameter analysis of lymph nodes still needs to be explored further.

Dual-energy CT can evaluate lymph nodes quantitatively. IC and NIC can reflect the difference in iodine contents of lymph nodes, and indirectly, their blood supply. λ_{HU} describes the dynamic change of CT values, and each tissue type has its characteristic HU slope of the curve[17,26]. Our study found that the IC and NIC values measured in the AP, PP, and DP were significantly higher in metastatic lymph nodes than in non-metastatic lymph nodes, and one explanation is that tumor cell invasion increases blood supply to lymph nodes[27]. We achieved a higher sensitivity with both IC and NIC in the PP, which is superior to conventional CT and PET/CT for HCC patients[16].

Both metastatic and non-metastatic lymph nodes followed descending spectrum curve patterns, but the curve pattern of the metastatic nodes was much steeper, suggesting that λ_{HU} could reflect different statuses of lymph nodes (metastatic or non-metastatic). The sensitivity of detecting malignant lymph nodes with λ_{HU} in the PP in our study is comparable to spectral CT in lung cancer[19,20] and colon cancer[20].

There was no statistically significant difference in the maximal short axis diameter of lymph nodes between patients with active hepatitis and non-active hepatitis in our study. Our result is different from that of Shu *et al*[10], and the possible reason may be due to different statuses of hepatitis and hepatic fibrosis[4,10,11]. The IC, NIC, and λ_{HU} values of non-metastatic lymph nodes in patients with active hepatitis were statistically higher than those in patients with non-active hepatitis in the PP, indicating that active hepatitis has an influence on regional lymph nodes, such as causing inflammation, resulting in increased blood flow and metabolism compared to normal lymph nodes[13,23]. There was no statistical difference in IC, NIC, or λ_{HU} values of metastatic lymph nodes between the active hepatitis group and non-active hepatitis group, suggesting that active hepatitis does not deteriorate the capabilities for detection and characterization of metastatic lymph nodes in HCC patients.

In our study, the parameters of dual energy CT (such as IC, NIC, and λ_{HU}) reliably identified the metastatic lymph nodes. The sensitivity and specificity of maximal short axis diameter combined with IC, NIC, or λ_{HU} values were higher than those of any single parameter (maximal short axis diameter, IC, NIC, or λ_{HU}) alone (IC: 84.5% and 83.0%, NIC: 86.9% and 93.6%, λ_{HU}: 86.2% and 89.8%, respectively). This indicates that

Table 2 Quantitative parameters [median (P25, P75)] for lymph nodes in patients with hepatocellular carcinoma complicated with active *vs* non-active hepatitis

		Metastatic			Non-metastatic		
		Active hepatitis (group *P1*)	Non-active hepatitis (group *P2*)	*P*-value	Active hepatitis (group *N1*)	Non-active hepatitis (group *N2*)	*P*-value
Maximal short axis diameter (cm)		1.50 (1.12, 2.00)	1.40 (0.90, 1.70)	0.058	0.70 (0.58, 0.90)	0.60 (0.50, 0.78)	0.083
IC (mg/mL)	AP	10.12 (7.63, 12.87)	11.02 (8.40, 13.68)	0.899	9.07 (6.35, 11.53)	7.73 (5.46, 9.58)	0.099
	PP	20.75 (18.40, 24.28)	18.83 (14.95, 21.31)	0.647	15.03(10.21, 18.02)	13.82 (10.40, 19.05)	0.001
	DP	14.19 (11.59, 17.47)	13.49 (10.53, 18.77)	0.793	19.65 (14.47, 22.62)	18.03 (13.78, 21.13)	0.908
NIC	AP	0.12 (0.08, 0.15)	0.11 (0.08, 0.14)	0.269	0.10 (0.07, 0.12)	0.10 (0.07, 0.13)	0.598
	PP	0.39 (0.27, 0.51)	0.34 (0.26, 0.43)	0.165	0.31 (0.23, 0.39)	0.19 (0.16, 0.26)	0.013
	DP	0.55 (0.42, 0.68)	0.51 (0.43, 0.65)	0.785	0.40 (0.35, 0.56)	0.35 (0.25, 0.44)	0.647
λ_{HU}	AP	0.62 (0.48, 0.82)	0.70 (0.53, 0.84)	0.195	0.49 (0.35, 0.64)	0.57 (0.40, 0.73)	0.161
	PP	1.45 (1.15, 1.67)	1.38 (0.89, 1.43)	0.73	0.95 (0.65, 1.16)	0.80 (0.68, 1.19)	0.002
	DP	1.23 (0.90, 1.44)	1.17 (1.01, 1.33)	0.812	0.91 (0.75, 1.11)	0.87 (0.66, 1.12)	0.726

IC: Iodine concentration; NIC: Normalized iodine concentration; λ_{HU}: Slope of the spectral curve; AP: Arterial phase; PP: Portal phase; DP: Delayed phase.

the presence of metastatic lymph nodes should be considered in patients with an enlarged lymph node (≥ 0.950 cm), especially when suspected spectral quantitative parameters were noted in a dual energy CT scan. Dual energy CT can provide more reliable information for the identification of benign and malignant lymph nodes than conventional CT.

There were some limitations in this study. First, this was a retrospective study and the population size of this study was relatively small. Second, lymph nodes with a maximal short axis size of less than 4.0 mm were excluded from the study due to the uncertainty of ROI measurements. Third, the absence of a comparison with MRI presents another limitation. Finally, the distinction between normal lymph nodes, metastatic lymph nodes, and inflammatory lymph nodes was not analyzed in our study, since it was not our main aim.

In conclusion, dual-energy CT contributes beneficially to regional lymph node assessment for HCC patients. A diagnosis combining analysis of maximal short axis diameter with IC, NIC, or λ_{HU} values is superior to using any single parameter alone. Active hepatitis does not deteriorate the capabilities for detection and characterization of metastatic lymph nodes.

Table 3 Cut-off values, area under the curve, sensitivity, and specificity of dual-energy computed tomography for metastatic *vs* non-metastatic lymph nodes in patients with hepatocellular carcinoma

Parameter		AUC	Cut-off value	Sensitivity, %	Specificity, %
Maximal short axis diameter(cm)		0.883	0.950	73.3	88.7
IC (mg/mL)	AP	0.697	9.845	68.6	72.0
	PP	0.902	18.060	81.9	82.4
	DP	0.755	16.005	73.6	76.9
NIC	AP	0.756	0.106	72.8	73.9
	PP	0.918	0.272	83.9	84.1
	DP	0.836	0.467	74.5	79.2
λ_{HU}	AP	0.755	0.582	73.8	75.6
	PP	0.889	1.098	81.8	84.1
	DP	0.836	1.077	78.1	79.0
Diameter + $\lambda_{HU\ (PP)}$		0.945	Combined diagnosis in parallel	86.2	89.8
Diameter + IC $_{(PP)}$		0.884		84.5	83.0
Diameter + NIC $_{(PP)}$		0.960		86.9	93.6

IC: Iodine concentration; NIC: Normalized iodine concentration; λ_{HU}: Slope of the spectral curve; AP: Arterial phase; PP: Portal phase; DP: Delayed phase.

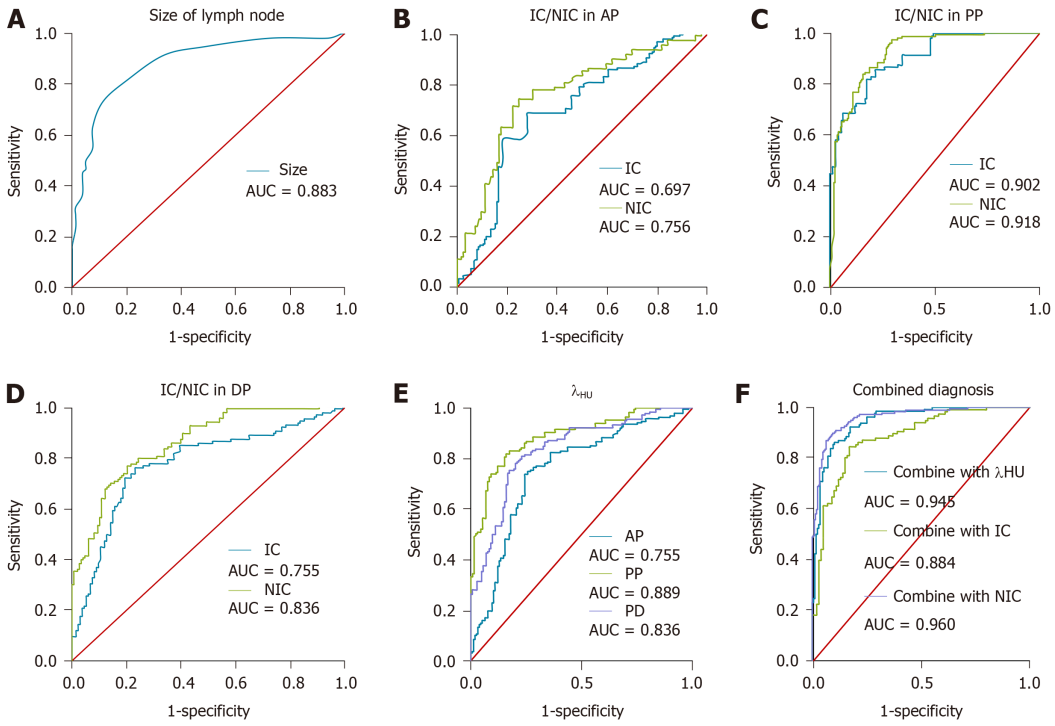

Figure 3 Receiver operating characteristic curve analysis of dual energy computed tomography quantitative parameters for metastatic and non-metastatic lymph nodes. A: Maximal short axis diameter of lymph nodes; B: Iodine concentration (IC)/normalized IC (NIC) in the arterial phase; C: IC/NIC in the portal phase; D: IC/NIC in the delayed phase; E: Slope of the spectral curve (λ_{HU}) in three contrast-enhanced phases; F: Combination of maximal short axis diameter of lymph nodes with λ_{HU}, IC, or NIC in the portal phase. IC: Iodine concentration; NIC: Normalized iodine concentration; λ_{HU}: Slope of the spectral curve; AP: Arterial phase; PP: Portal phase; DP: Delayed phase.

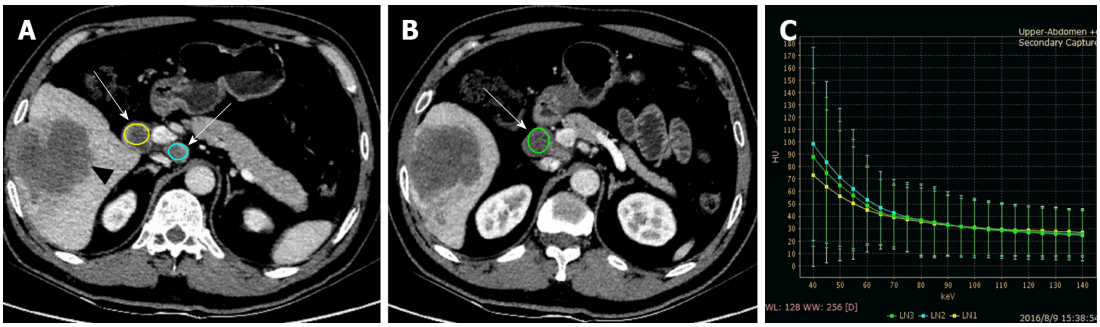

Figure 4 A 44-year-old male with hepatocellular carcinoma and lymph node metastasis. A and B: Region of interest was placed in the maximal axial section for lymph nodes (white arrow); C: The spectrum curve of the removed lymph nodes in the portal phase showed a descending curve with a slope of about 1.0-1.7. The iodine concentrations of the three lymph nodes were 20.01 mg/mL, 21.06 mg/mL, and 22.50 mg/mL, respectively. The normalized iodine concentrations were 0.41, 0.53, and 0.64, respectively.

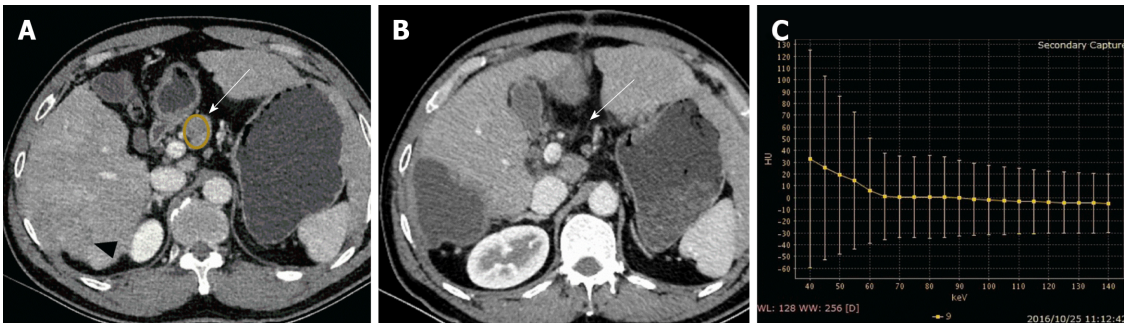

Figure 5 A 31-year-old male with hepatocellular carcinoma and non-metastatic lymph nodes. A: Region of interest was placed in the maximal axial section for lymph nodes (white arrow); B: Postoperative computed tomography showed that the lymph node was removed (white arrow); C: The spectrum curve of the removed lymph node in the portal phase showed a descending curve with a slope of about 0.8. The iodine concentration of the lymph node was 12.20 mg/mL. The normalized iodine concentration was 0.83.

ARTICLE HIGHLIGHTS

Research background

Regional lymph node metastasis in patients with hepatocellular carcinoma (HCC) is not uncommon, and is often under- or misdiagnosed. Regional lymph node metastasis is associated with a negative prognosis in patients with HCC, and surgical resection of lymph node metastasis is considered feasible and efficacious in improving the survival and prognosis. It is critical to characterize lymph node preoperatively. There is currently no consensus regarding the optimal method for the assessment of regional lymph nodes in patients with HCC.

Research motivation

Dual-energy computed tomography (CT) can provide quantitative information with monochromatic spectral images, material decomposition images, spectrum curves, and effective atomic number images. The role of dual-energy CT parameters in the evaluation of malignant lymph nodes has been reported with excellent results. However, there have been no dual-energy CT studies regarding lymph node assessment in HCC.

Research objectives

The main objective of our study was to evaluate the diagnostic value of dual energy CT parameters [such as iodine concentrations (IC), normalized IC (NIC), and slope of the spectral curve (λ_{HU})] in regional lymph node assessment for HCC patients.

Research methods

In this retrospective study, a total of 156 lymph nodes (33 patients with 104 non-metastatic and 10 patients with 52 metastatic) from 43 patients were finally included. According to the lymph node status, the lymph nodes were divided into group *P* (52 metastatic) and group *N* (104 non-metastatic). According to the active hepatitis diagnosis standard, the lymph nodes in groups *P* and *N* were further divided into an active hepatitis group (group *P1*, $n = 34$; group *N1*, $n = 73$) and a non-active hepatitis group (group *P2*, $n = 18$; group *N2*, $n = 31$), respectively. All patients underwent three-phase dual-energy CT scan preoperatively [arterial phase (AP), portal phase (PP), and delayed phase (DP)]. The maximal short axis diameter (MSAD), IC, NIC, and λ_{HU} of each group in the AP, PP, and DP were analyzed.

Research results

The MSAD, IC, NIC, and λ_{HU} showed statistical differences between groups *P* and *N* ($P < 0.05$ for all) in dual-energy CT scans in all the three phases. The diagnostic value of IC, NIC, and λ_{HU} in the PP to distinguish benign from metastatic lymph nodes was the best among the three phases (AP, PP, and DP), with a sensitivity up to 81.9%, 83.9%, and 81.8%, and specificity up to 82.4%, 84.1% and 84.1%, respectively. To distinguish benign from metastatic lymph nodes, the diagnostic value of combined analyses of MSAD with IC, NIC, or λ_{HU} in PP was superior to the dual energy CT parameters alone, with a sensitivity up to 84.5%, 86.9%, and 86.2%, and a specificity up to 83.0%, 93.6% and 89.8%, respectively. Between groups *P1* and *P2* and groups *N1* and *N2*, only IC, NIC, and λ_{HU} between groups *N1* and *N2* in the PP had a statistically significant difference ($P < 0.05$).

Research conclusions

Dual-energy CT parameters (IC, NIC, and λ_{HU}) are sensitive and specific, and can help to differentiate benign from metastatic lymph nodes in patients with HCC, especially in PP CT scans. The diagnostic efficacy of combined analysis of MSAD with IC, NIC, or λ_{HU} values is superior to using any single parameter alone. Active hepatitis does not deteriorate the capabilities for characterization of metastatic lymph nodes.

Research perspectives

The future direction in this field will probably focus on the comparison of diagnostic efficacy of different imaging methods to differentiate benign from metastatic lymph nodes in patients with HCC, *e.g.*, between dual-energy CT and magnetic resonance imaging.

REFERENCES

1 **Tomimaru Y**, Wada H, Eguchi H, Tomokuni A, Hama N, Kawamoto K, Marubashi S, Umeshita K, Doki Y, Mori M, Wakasa K, Nagano H. Clinical significance of surgical resection of metastatic lymph nodes from hepatocellular carcinoma. *Surg Today* 2015; **45**: 1112-1120 [PMID: 25205550 DOI: 10.1007/s00595-014-1028-8]

2 **Xiaohong S**, Huikai L, Feng W, Ti Z, Yunlong C, Qiang L. Clinical significance of lymph node metastasis in patients undergoing partial hepatectomy for hepatocellular carcinoma. *World J Surg* 2010; **34**: 1028-1033 [PMID: 20174806 DOI: 10.1007/s00268-010-0400-0]

3 **Xia F**, Wu L, Lau WY, Li G, Huan H, Qian C, Ma K, Bie P. Positive lymph node metastasis has a marked impact on the long-term survival of patients with hepatocellular carcinoma with extrahepatic metastasis. *PLoS One* 2014; **9**: e95889 [PMID: 24760012 DOI: 10.1371/journal.pone.0095889]

4 **Kobayashi S**, Takahashi S, Kato Y, Gotohda N, Nakagohri T, Konishi M, Kinoshita T. Surgical treatment of lymph node metastases from hepatocellular carcinoma. *J Hepatobiliary Pancreat Sci* 2011; **18**: 559-566 [PMID: 21331804 DOI: 10.1007/s00534-011-0372-y]

5 **Wu X**, Li B, Qiu J, Shen J, Zheng Y, Li Q, Liao Y, He W, Zou R, Yuan Y. Hepatectomy Versus Hepatectomy With Lymphadenectomy in Hepatocellular Carcinoma: A Prospective, Randomized Controlled Clinical Trial. *J Clin Gastroenterol* 2015; **49**: 520-528 [PMID: 25564411 DOI: 10.1097/MCG.0000000000000277]

6 **Hashimoto M**, Matsuda M, Watanabe G. Metachronous resection of metastatic lymph nodes in patients with hepatocellular carcinoma. *Hepatogastroenterology* 2009; **56**: 788-792 [PMID: 19621703]

7 **Grobmyer SR**, Wang L, Gonen M, Fong Y, Klimstra D, D'Angelica M, DeMatteo RP, Schwartz L, Blumgart LH, Jarnagin WR. Perihepatic lymph node assessment in patients undergoing partial hepatectomy for malignancy. *Ann Surg* 2006; **244**: 260-264 [PMID: 16858189 DOI: 10.1097/01.sla.0000217606.59625.9d]

8 **Kim HJ**, Cho A, Yun M, Kim YT, Kang WJ. Comparison of FDG PET/CT and MRI in lymph node staging of endometrial cancer. *Ann Nucl Med* 2016; **30**: 104-113 [PMID: 26546334 DOI: 10.1007/s12149-015-1037-8]

9 **Kim RD**, Reed AI, Fujita S, Foley DP, Mekeel KL, Hemming AW. Consensus and controversy in the management of hepatocellular carcinoma. *J Am Coll Surg* 2007; **205**: 108-123 [PMID: 17617340 DOI: 10.1016/j.jamcollsurg.2007.02.025]

10 **Shu J**, Zhao JN, Han FG, Tang GC, Luo YD, Luo L, Chen X. Chronic hepatitis B: Enlarged perihepatic lymph nodes correlated with hepatic histopathology. *World J Radiol* 2013; **5**: 208-214 [PMID: 23805371 DOI: 10.4329/wjr.v5.i5.208]

11 **Schreiber-Dietrich D**, Pohl M, Cui XW, Braden B, Dietrich CF, Chiorean L. Perihepatic lymphadenopathy in children with chronic viral hepatitis. *J Ultrason* 2015; **15**: 137-150 [PMID: 26676184 DOI: 10.15557/JoU.2015.0012]

12 **Seber T**, Caglar E, Uylar T, Karaman N, Aktas E, Aribas BK. Diagnostic value of diffusion-weighted magnetic resonance imaging: Differentiation of benign and malignant lymph nodes in different regions of the body. *Clin Imaging* 2015; **39**: 856-862 [PMID: 26091745 DOI: 10.1016/j.clinimag.2015.05.006]

13 **Lee JE**, Jang JY, Jeong SW, Lee SH, Kim SG, Cha SW, Kim YS, Cho YD, Kim HS, Kim BS, Jin SY, Choi DL. Diagnostic value for extrahepatic metastases of hepatocellular carcinoma in positron emission tomography/computed tomography scan. *World J Gastroenterol* 2012; **18**: 2979-2987 [PMID: 22736922 DOI: 10.3748/wjg.v18.i23.2979]

14 **Choi EK**, Yoo IeR, Park HL, Choi HS, Han EJ, Kim SH, Chung SH, O JH. Value of Surveillance (18)F-FDG PET/CT in Colorectal Cancer: Comparison with Conventional Imaging Studies. *Nucl Med Mol Imaging* 2012; **46**: 189-195 [PMID: 24900059 DOI: 10.1007/s13139-012-0145-9]

15 **Nakagawa T**, Yamada M, Suzuki Y. 18F-FDG uptake in reactive neck lymph nodes of oral cancer: Relationship to lymphoid follicles. *J Nucl Med* 2008; **49**: 1053-1059 [PMID: 18587087 DOI: 10.2967/jnumed.107.049718]

16 **Ho CL**, Chen S, Yeung DW, Cheng TK. Dual-tracer PET/CT imaging in evaluation of metastatic hepatocellular carcinoma. *J Nucl Med* 2007; **48**: 902-909 [PMID: 17504862 DOI: 10.2967/jnumed.106.036673]

17 **Marin D**, Boll DT, Mileto A, Nelson RC. State of the art: Dual-energy CT of the abdomen. *Radiology* 2014; **271**: 327-342 [PMID: 24761954 DOI: 10.1148/radiol.14131480]

18 **Rizzo S**, Radice D, Femia M, De Marco P, Origgi D, Preda L, Barberis M, Vigorito R, Mauri G, Mauro A, Bellomi M. Metastatic and non-metastatic lymph nodes: Quantification and different distribution of iodine uptake assessed by dual-energy CT. *Eur Radiol* 2018; **28**: 760-769 [PMID: 28835993 DOI: 10.1007/s00330-017-5015-5]

19 **Baxa J**, Vondráková A, Matoušková T, Růžičková O, Schmidt B, Flohr T, Sedlmair M, Ferda J. Dual-phase dual-energy CT in patients with lung cancer: Assessment of the additional value of iodine quantification in lymph node therapy response. *Eur Radiol* 2014; **24**: 1981-1988 [PMID: 24895031 DOI: 10.1007/s00330-014-3223-9]

20 **Al-Najami I**, Lahaye MJ, Beets-Tan RGH, Baatrup G. Dual-energy CT can detect malignant lymph nodes in rectal cancer. *Eur J Radiol* 2017; **90**: 81-88 [PMID: 28583651 DOI: 10.1016/j.ejrad.2017.02.005]

21 **Al-Najami I**, Beets-Tan RG, Madsen G, Baatrup G. Dual-Energy CT of Rectal Cancer Specimens: A CT-based Method for Mesorectal Lymph Node Characterization. *Dis Colon Rectum* 2016; **59**: 640-647 [PMID: 27270516 DOI: 10.1097/DCR.0000000000000601]

22 **Liang H**, Li A, Li Y, Cheng H, Zhao Q, Li J, Wang Q. A retrospective study of dual-energy CT for clinical detecting of metastatic cervical lymph nodes in laryngeal and hypopharyngeal squamous cell carcinoma. *Acta Otolaryngol* 2015; **135**: 722-728 [PMID: 25719763 DOI: 10.3109/00016489.2015.1015164]

23 **Tawfik AM**, Razek AA, Kerl JM, Nour-Eldin NE, Bauer R, Vogl TJ. Comparison of dual-energy CT-derived iodine content and iodine overlay of normal, inflammatory and metastatic squamous cell carcinoma cervical lymph nodes. *Eur Radiol* 2014; **24**: 574-580 [PMID: 24081649 DOI: 10.1007/s00330-013-3035-3]

24 **Sano T**. Evaluation of the gastric cancer treatment guidelines of the Japanese Gastric Cancer Association. *Gan To Kagaku Ryoho* 2010; **37**: 582-586 [PMID: 20414011 DOI: 10.1007/s10120-011-0042-4]

25 **Chinese Society of Contagious Disease and Parasitic Disease, Chinese Society of Hepatology**. Chinese Medical Association (2001) Guideline: prevention and treatment of viral hepatitis. *Zhonghua Chuanranbing Zazhi* 2001; **19**: 56-62 [DOI: 10.3760/j.issn:1000-6680.2001.01.027]

26 **Kim S**, Shuman WP. Clinical Applications of Dual-Energy Computed Tomography in the Liver. *Semin Roentgenol* 2016; **51**: 284-291 [PMID: 27743564 DOI: 10.1053/j.ro.2016.05.019]

27 **Pant V**, Sen IB, Soin AS. Role of ^{18}F-FDG PET CT as an independent prognostic indicator in patients with hepatocellular carcinoma. *Nucl Med Commun* 2013; **34**: 749-757 [PMID: 23689586 DOI: 10.1097/MNM.0b013e3283622eef]

Published By Baishideng Publishing Group Inc
7041 Koll Center Parkway, Suite 160, Pleasanton, CA 94566, USA
Telephone: +1-925-2238242
Fax: +1-925-2238243
E-mail: bpgoffice@wjgnet.com
Help Desk:http://www.f6publishing.com/helpdesk
http://www.wjgnet.com